

**Development of the Control System for the Motor-driven
Electromechanical Total Artificial Heart**

Hee Chan Kim^o, Sang Hun Lee, Jong Won Kim,
Jin Tae Kim, Byoung Goo Min

Department of Control and Instrumentation,
College of Engineering, and
Department of Biomedical Engineering,
College of Medicine,
Seoul National University

ABSTRACT

A micro-processor based control system for a brushless DC motor used in the motor-driven electromechanical total artificial heart was developed. Functionally, the control system is composed of two parts. The first part is the velocity and position controller to assure that the motor follows a predetermined optimal velocity profile with minimal energy consumption, and to guarantee the full stroke length. This part also utilize the passive adaptive control method to be robust against the load disturbance, system parameter variation, and uncertainty which is the environment of artificial heart system.

The pump output control is the second part, and this part provides the required responses of the artificial heart to the time-varying physiologic demands. The basic requirements of these responses are preload sensitivity, afterload insensitivity, and the balanced ventricular outputs. The performance and reliability of this control system was evaluated through a series of mock circulation tests and animal implantation, and the results are very encouraging.

I. INTRODUCTION

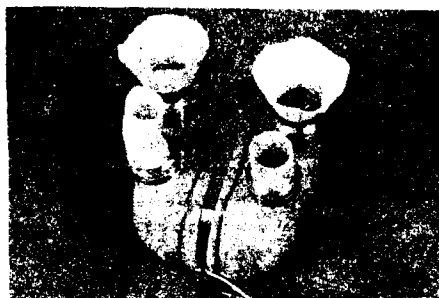
Since the first human implantation in Dec. 1982 [1], the artificial heart has been used as permanent substitute and as bridge prior to transplantation. Based upon this clinical usage of the pneumatic type artificial heart, the possibility of long-term survival is expected within ten years[2].

However, the present pneumatic artificial heart has significant disadvantages for clinical use due to its bulky external air compressor and control unit and the percutaneous air tubes. These two large-bore-size air and vacuum tubes

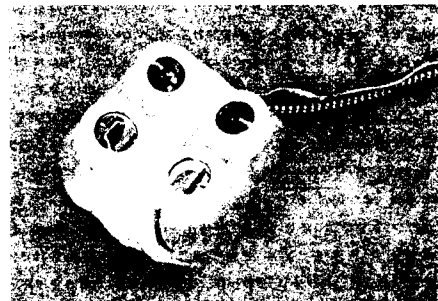
pose significant problems of infection, and have been an impetus to develop a totally portable artificial heart[3].

Compared to the conventional air-driven total artificial heart, the motor-driven artificial heart has several advantages, such as portable system, usage of small-diameter wire instead of large size percutaneous tubes, possibilities of accurate control and quiet operation. Also, the use of electricity as energy source for pumping is expected to lead us to the era of tether-free totally implantable artificial heart in the near future. The developments in microelectronics, permanent magnet material, rechargeable battery, and transcutaneous energy transmission (TET) technique, make the permanent artificial heart as more realistic goal [4].

An unique and efficient moving-actuator mechanism using circularly rolling-cylinder which optimally utilize the dead space between artificial ventricles and partially solve the fitting problems, as shown in the Fig. 1, was achieved[5]. The control system of this new type motor-driven artificial heart was also developed and it is functionally divided into two parts. The first part is the velocity and position controller to assure that the motor follows a predetermined optimal velocity profile with minimal energy consumption, and to guarantee the full stroke length. Because the batteries and TET which will supply the whole required energy have the limited storage capacities and transmitted peak power, it is essential to drive the motor in a fashion that minimizes electric power consumption.[6] This part also utilize the passive adaptive control method to be robust against the load disturbance, system parameter variation, and uncertainty which is the typical operating environment of artificial heart system.



(a)



(b)

Fig. 1. Figures of the developed motor-driven rolling-cylinder type total artificial heart (a) linear, (b) circular type.

The pump output control is the second part, and this part provides the required responses of the artificial heart to the time-varying physiologic demands. The basic requirements of these responses are preload sensitivity, afterload insensitivity, and the balanced ventricular outputs.

After the long-term mock circulation tests for the evaluation of performance and reliability, the first animal implantation was performed with a female calf. She survived for 100 hours with a good physical condition as voluntarily standing up and eating[5]. Our control algorithm performed by manual adjustment worked well, as shown by the almost normal ranges of hemodynamic and laboratory data during implantation.

II. Velocity and Position Control System

In the motor control system for artificial heart, both of the velocity and position control are required. Minimum energy consumption and the reduction of the reactive inertial forces are the main objectives of the velocity control system. The position control is required to guarantee the maximum stroke volume as well as stable operation[7] and to instantaneously control the stroke volume of each ventricles which will be used in the pump output control to provide the balanced ventricular outputs. The difficulties in the design of these control systems arise from the following factors. Firstly, the frictional load of motor varies not only within each ejection period but also according to the changes of the physiologic state. Secondly, other load-related parameters such as torque constant(Kt), inertia(Jm), viscous frictional coefficient(Bm), and the mechanical efficiency of total pump system are very difficult to measure their nominal values and varies themselves due to the deterioration of rubrication, wear of the mechanical parts, and/or the temperature increase.

2.1 Optimal Velocity Profile

A state space model for a brushless DC motor is given by,

$$\frac{d}{dt} \begin{bmatrix} \Theta \\ w \\ i \end{bmatrix} = \begin{bmatrix} 0 & 1 & 0 \\ 0 & -B_m/J_m & K_t/J_m \\ 0 & -K_e/L & -R/L \end{bmatrix} \begin{bmatrix} \Theta \\ w \\ i \end{bmatrix} + \begin{bmatrix} 0 \\ 0 \\ 1/L \end{bmatrix} E_m + \begin{bmatrix} 0 \\ -1/J_m \\ 0 \end{bmatrix} \frac{T}{L} \quad (1)$$

Generally the inductance term(L) of a DC motor is negligible and in our artificial heart system, the frictional load linearly increases from zero to the maximum value during ejection period as follows,

$$L \frac{di}{dt} = 0 \quad \text{and}$$

$$T = \frac{P_{lvmax}}{\Theta_{max}} \times C \times \Theta \quad [N-m] \quad (2)$$

where P_{lvmax} [mmHg] is the systolic peak aortic pressure, Θ_{max} [rad] is the maximum rotational angle, C [N-m/mmHg] is a conversion constant, and Θ [rad] is a rotational angle. Based upon these two assumptions, the resultant simplified expression of the system is given by,

$$\frac{d}{dt} \begin{bmatrix} \Theta \\ w \end{bmatrix} = \begin{bmatrix} 0 & 1 \\ -P_{lvmax}C/J_m\Theta_{max} & -K_tK_e/RJ_m - B_m/J_m \end{bmatrix} \times \begin{bmatrix} \Theta \\ w \end{bmatrix} + \begin{bmatrix} 0 \\ K_t/RJ_m \end{bmatrix} E_m \quad (3)$$

$$\text{with } \begin{bmatrix} \Theta(0) \\ w(0) \end{bmatrix} = \begin{bmatrix} 0 \\ 0 \end{bmatrix} \text{ and } \begin{bmatrix} \Theta(tf) \\ w(tf) \end{bmatrix} = \begin{bmatrix} 58.89 \\ 0 \end{bmatrix}$$

The process described by the above state equation is to be controlled to minimize the performance measure of the energy consumption,

$$J(E_m(t)) = \int_0^{tf} (E_m(t) * i(t)) dt \quad (4)$$

The results of the numeric analysis of the optimal velocity profiles are shown in the Fig. 2 where the inertia(Jm), viscous frictional coefficient(Bm), and the maximum value of frictional load(Plvmax) vary in the reasonable ranges. As a whole, the optimal velocity profiles significantly differ from each other according to the changes of these load parameters.

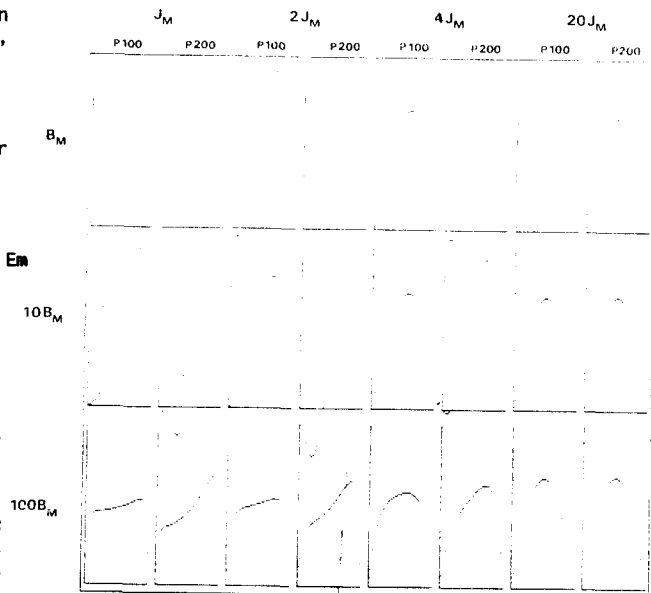


Fig. 2. Optimal velocity profiles under the variations of inertia ($J_m = 1.387e-5$ [N-m/sec²]), viscous frictional coefficient ($B_m = 7.06e-6$ [N-m/rad/sec]), and frictional load ($P_{lvmax} = 100, 200$ [mmHg]).

2.2 Passive Adaptive Control

The variety of the optimal velocity profiles according to the load disturbance and the perturbations in the system parameters makes it almost impossible to implement the optimal controller to provide the minimum energy consumption. In this paper, the passive adaptive control method was used to overcome this problem in determining the optimal velocity profile[8]. An adaptive control system is effective in the case of the plant system varies significantly from its nominal values and/or its nominal values themselves are not exactly known[9]. The basic structure of this passive adaptive control system is shown in the Fig. 3, where $P(s)$ is a plant, $P_m(s)$ is the model which represents the nominal state of $P(s)$, and the compensator $H(s)$.

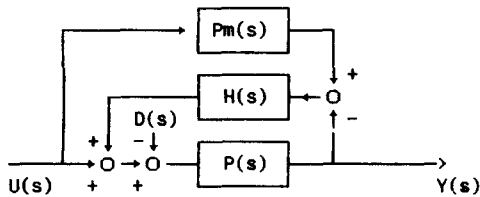


Fig. 3. Basic structure of passive adaptive control system

If we select $H(s)$ as the inverse system of $P_m(s)$ multiplied by the high gain β , the transfer functions of input $U(s)$ and disturbance $D(s)$ to output $Y(s)$ becomes as follows,

$$W(s) = \frac{Y(s)}{U(s)} = \frac{1 + \beta}{P_m(s)/P(s) + \beta} P_m(s) \quad (5)$$

$$V(s) = \frac{Y(s)}{D(s)} = \frac{1 + \beta}{P_m(s)/P(s) + \beta} P(s) \frac{-1}{1 + \beta} \quad (6)$$

respectively. Therefore, as increasing the compensator gain β , the transfer function $W(s)$ converges to the model $P_m(s)$ and $V(s)$ to zero as follows,

$$W(s) = \frac{Y(s)}{U(s)} \rightarrow P_m(s) \quad (7)$$

$$V(s) = \frac{Y(s)}{D(s)} \rightarrow 0 \quad (8)$$

Also, the sensitivity of $W(s)$ to the perturbations in the system parameters can be reduced by increasing β .

$$S = \frac{1}{W(s)} \frac{dW(s)}{d\beta} \rightarrow 0, \quad \beta \gg 1 \quad (9)$$

The computer simulation results are shown in the Fig. 4, where both of the load disturbance and the system parameters perturbation are artificially generated.

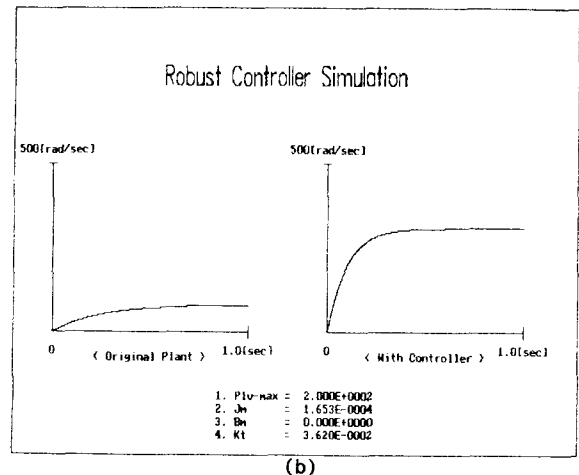
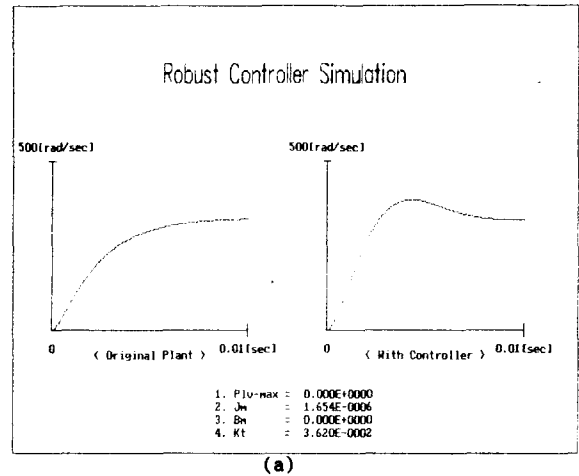


Fig. 4. Comparison of the step responses of the original plant with and without passive adaptive controller under (a) no load, and (b) $P1v_{max}=200[\text{mmHg}]$ conditions.

2.3 Proposed Control System

The proposed motor control system is shown in the Fig. 5, where the passive adaptive controller makes the total system always behave in nominal state under the load disturbance and the system parameters perturbation. Then, the single optimal velocity profile for this nominal system is used to provide the minimum energy consumption. Also, the conventional PID(Proportional Integral and Derivative) controller is included to improve the response characteristics of the velocity controller, and the tuning of the PID gains is performed independently because there's no interference between two controllers, that is, two-degrees-of-freedom control system. To make the position control certain, the reference optimal velocity command is generated as a function of the position. In Fig. 6, the waveforms of the response of control system with the input voltage and current are shown.

In-vitro tests have verified the usefulness of our control algorithm which produced a sensitive cardiac output response to preload and independency of pump output to afterload. The cardiac output response to these physiologic variations is shown in Figures 8 and 9 where cardiac output(C.O.), heart rate(H.R.) and left atrial pressure(LAP) are both plotted against right atrial pressure(RAP). With a rise in RAP from 0 to 6 mmHg, the cardiac output increased from approximately 4 L/min to about 9 L/min, while the heart rate is increased from 60 to 120 BPM. The afterload independency of pump output is also shown in the same figures where the cardiac output response curve does not change regardless of the changes of aortic pressure within three values of 80, 100, and 120 mmHg.

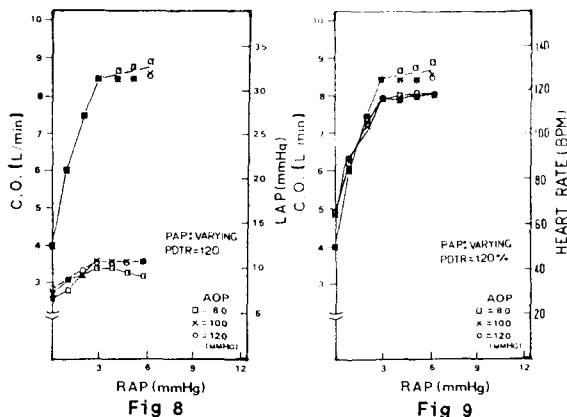


Fig. 8. Cardiac output and left atrial pressure responses against the changes of right atrial pressure as preload changes.

Fig. 9. Changes of heart rate against the preload variations to achieve the cardiac output response shown in Fig. 8.

Also the results of mock circulation experiments demonstrated that there exists a closely matched values between right and left atrial pressures. As shown in Fig. 10, the strategy of controlling percent diastolic time ratio (PDTR) works well, and together with the different sac volumes, we can obtain the balanced outputs of two ventricles.

4.2 In-vivo Experiments

In-vivo test as an extracorporeal biventricular assist device on two sheeps gave us another confirmation on the possibility of chronic animal implant. In animal implantation, "Shim Chung"(female calf, 4 month old, 100Kg) recovered after surgery to a degree of voluntarily standing and eating, and survived for 100 hours in excellent physical condition(Fig. 11). The main cause of death was an acute pulmonary edema induced by accidental pump's failure. The cause of this failure was the electrical short circuit at intermediate connector pins by the permeated body fluid.

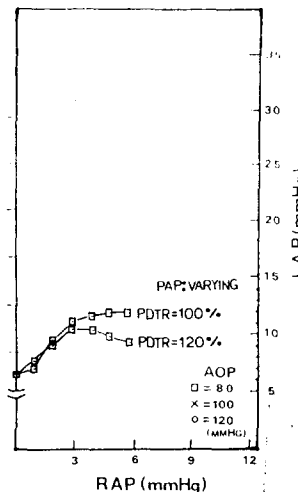


Fig. 10. Left atrial pressure response against the preload changes with the different percent diastolic time ratio (PDTR) where increase of LAP is suppressed as increase of RAP by larger PDTR.

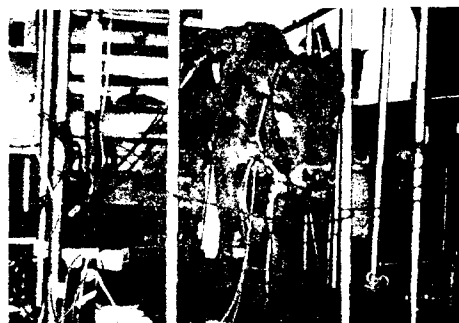


Fig. 11. "Shim Chung", a female calf, 4 months old, approximately 100Kg who received a circular type artificial heart for 100 hours.

The variation of hemodynamic parameters of AoP, PAP, RAP, LAP, and heart rate are shown in Fig.12 for survival period. A typical waveform of them is shown in Fig. 13. Higher RAP and LAP, as shown in Fig. 12, may be caused by the posture of animal, where the animal's weight press the atrial cuffs down to produce unbalanced pressures inside atrial cuffs. But during standing phase, a normal, well-balanced condition between LAP and RAP was restored as marked in the same Figure.

The parameter adjustment on controller system was required frequently only on the first day after surgery, and, in this case, the heart rate was adjusted to maintain LAP within physiological limit. A negative suction pressure was provided into the variable volume inside pump to help diastolic fulfillment of blood sac, when LAP was higher than 30 mmHg. A vacuum connected through water column was used to maintain constant suction pressure of -10 mmHg.

After death, an close autopsy was performed; some thrombo-emboli in both lungs and kidneys were found, the state of liver was fairly good. The probable origin of the thrombo-emboli was considered to be the quick-connector region. The atrial cuffs were slightly folded and looked like to be pressed down by the animal's weight.

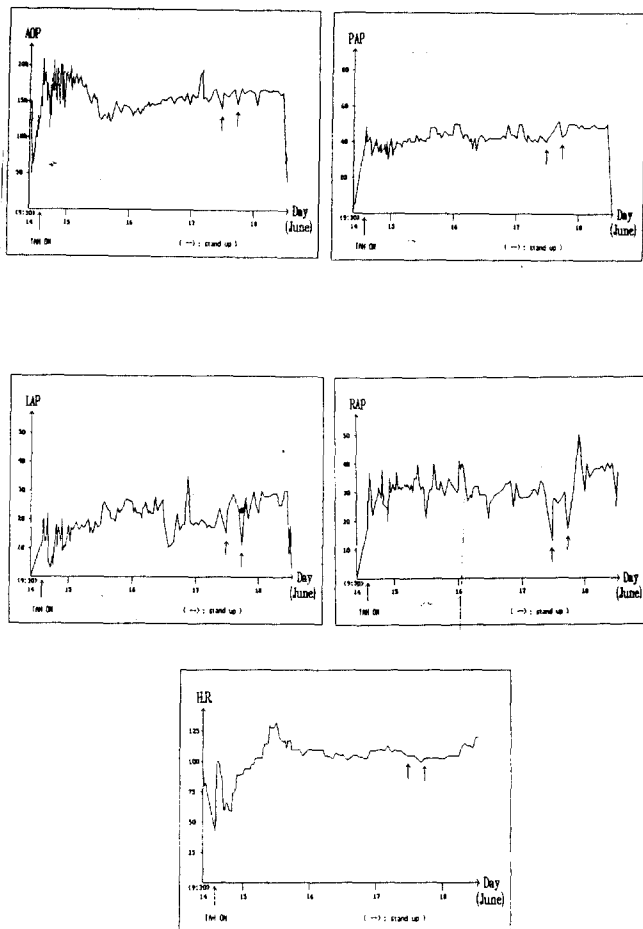


Fig. 12. Variations of the measured hemodynamic parameters of aortic(AoP), pulmonary arterial(PAP), left atrial(LAP), and right atrial(RAP) pressures, and heart rate(HR).

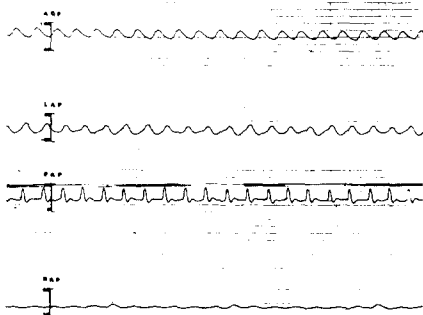


Fig. 13. Typical waveforms of the results of animal experiment.

V. Discussion

The control system for the brushless DC motor-driven total artificial heart was developed. To achieve the minimum energy consumption, the optimal velocity profile for

nominal plant was used where the passive adaptive controller made the whole system to be robust against the load disturbance and the system parameter perturbation. Also, a PID controller designed by a two-degree-of-freedom method was tuned to satisfy the specifications of response of the velocity controller. The validity of the proposed motor control system was shown by the stable operation under the parameter variations and the frictional load torque disturbance and the amount of the input power.

To provide the adequate cardiac output response to the time-varying physiological demand, the pump output control algorithm was also developed and it satisfied the basic three requirements on the pump output response through the mock circulation tests. The results of the animal implantation reconfirmed the availability of the overall artificial heart system.

References

- [1] W.C. Devris, J.L. Anderson, L.D. Joce, et.al., "Clinical Use of the Total Artificial Heart," *N. Eng. J. Med.* 310(5), pp 273-278, 1984.
- [2] W.S. Pierce, "Artificial Hearts and Blood Pumps in the Treatment of Profound Heart Failure," *Circulation* 68(4), pp 883-888, 1983.
- [3] R.K. Jarvik, "The Total Artificial Heart," *Sci. Amer.*, pp 74-80, Jan. 1981.
- [4] W.S. Pierce, "The Artificial Heart - 1986: Partial Fulfillment of a Promise," *Vol. XXXII Trans. Am. Soc. Artif. Intern. Organs*, pp 5-10, 1986.
- [5] B.G. Min, H.C. Kim, G.J. Cheon, J.W. Choi, K.H. Ryu, K.P. Seo, H. Ahn, and D.B. Olsen, "A Moving-Actuator Type Electromechanical Total Artificial Heart - Part II: Circular Type and Animal Experiments," *IEEE Trans. Biomed. Eng. in Review*.
- [6] U. Tsach, D.B. Geselowitz, A. Sinha, J. Tirinato, H.K. Hsu, G. Rosenberg, and W.S. Pierce, "Minimum Power Consumption of the Electric Ventricular Assist Device Through the Design of an Optimal Output Controller," *Vol. XXXIII Trans. Am. Soc. Artif. Intern. Organs*, pp 714-719, 1987.
- [7] G. Rosenberg, A.J. Snyder, W. Weiss, D.L. Landis, D.B. Geselowitz, and W.S. Pierce, "A Cam-Type Electric Motor-Driven Left Ventricular Assist Device," *Trans. of ASME*, Vol. 104, pp 214-220, Aug. 1982.
- [8] K. Tamaki, K. Ohnishi, and K. Miyachi, "Microprocessor-used Robust Control of DC Servo Motor by means of Passive Adaptive Control," *IEEE IECON'85*, pp 211-256, 1985.
- [9] Y. Dote, "Application of Modern Control Techniques to Motor Control," *Proc. of IEEE*, Vol.76, No. 4, pp 438-454, 1988.
- [10] A.P. Lioi, J.L. Orth, K.R. Crump, G. Diffie, P.A. Dew, S.D. Nielson, and D.B. Olsen, "In Vitro Development of Automatic Control for the Actively Filled Electrohydraulic Heart," *Artificial Organs*, 12(2), pp 152-162, 1988.
- [11] A.C. Guyton, C.E. Jones, T.C. Coleman, *Circulatory Physiology: Cardiac Output and its Regulation*, Philadelphia: WB Saunders, 1973.